Lanthanide Complexes as Molecular Dopants for Realizing Air-stable n-type Graphene Logic Inverters With Symmetric Transconductance

Ashwini S. Gajarushi,[#] Mohd Wasim,[#] Rizwan Nabi, Srinivasu Kancharlapalli, V. Ramgopal Rao, Gopalan Rajaraman, Chandramouli Subramaniam* and Maheswaran Shanmugam**

Materials and Methods

$La(NO_3)_3.6H_2O$ and $Ce(NO_3)_3.6H_2O$ were purchased from Alfa Aesar and used without any further purification. o-phenylenediammine (PD) was purchased from Sigma Aldrich and sublimed before use. 2,6-pyridinedicarboxaldehyde (PC) was prepared by oxidation of 2,6-Lutidine with selenium dioxide (SeO_2) according to reported method.[1] Detail synthetic procedure of **1** and **2** is given (scheme S1). **1** and **2** were crystallized by the slow diffusion of diethyl ether in their solution in dimethylformamide (DMF; CCDC number: 1849130-1849131). The single X-ray diffraction data of **1** and **2** were collected through Rigaku Saturn 724+ (Mo K_α) Single Crystal X-ray diffractometer. The elemental analysis of **1** and **2** were done through CHNS Analyser (ThermoQuest). The solution of crystalline solid of **1** and **2** in acetonitrile solvent was made by stirring it in distilled solvent for 3-4 h and the concentration of the solution was determined by Inductively coupled plasma atomic emission spectroscopy (ICP-AES) (Spectroanalytical instruments GmbH, ARCOS). The stability of the complex **1** and **2** in acetonitrile was determined by MALDI-ToF mass spectrometer (recorded by Bruker Autoflex speed, processed and simulated by Flux Analysis software). Atomic force microscopy (AFM) was done using MFP-3D Origin, Oxford Instruments in non-contact mode with Silicon Nitride tip. KPFM measurements was carried out on the same instrument with Asyelec.01-R2 Ti-Ir tips with 4.9 eV as work function. Zeiss ultra 55 FE-SEM was used for secondary electron microscopy. Micro-Raman spectroscopy of GFETs was carried out using Witec Alpha 300 RAS system, with 532 nm excitation laser and spectrally dispersed

over 1800 grooves/mm grating on to a Peltier cooled CCD. X-ray photoelectron spectroscopy was done using PHI 5000 Versa Probe – II (Al K_α: 1486 eV). The current voltage characterization for the GFETs and inverters were obtained using a 4-probe electrical work station (Suss Microtec) fitted with tungsten probe-tips (diameter 14 micron). A semiconductor parametric analyser (Agilent B1500A) was used for both to input voltage bias and measuring output current of GFET or output voltage of inverter. The methodology used, optimized energy and other details related to computational calculations are provided in ESI.

Synthetic procedure for $[LaL_1(NO_3)_3]$ (1)

A methanolic solution of $La(NO_3)_3.6H_2O$ (0.1000 g, 0.23 mmol) and 2,6 pyridine dicarboxaldehyde (PC) (0.0622 g, 0.46 mmol) in 15 mL of dry methanol was stirred for 10 minutes under N_2 atmosphere. Into that solution of o-phenylenediamine (PD) (0.0497 g, 0.46 mmol, 20 mL of dry methanol) was added slowly. The resultant reaction mixture was refluxed for 8 h. After completion, the reaction mixture was concentrated to 2 mL by evaporation of solvent through rotary evaporator. The precipitate was collected and dissolved in DMF. X-ray quality, yellow single crystals were obtained after 2-3 days upon diffusing diethyl ether under ambient conditions. Yield: 0.0190 g, 10.91%. Elemental anal. calcd. : C, 42.24; H, 2.45; N, 17.05; found: C, 41.66; H, 2.35; N 17.17. MALD-ToF-MS: m/z calcd for $C_{26}H_{19}N_9O_9La$ $[M+H]^+$ 740.036; found : 740.066

Synthetic procedure for $[CeL_1(NO_3)_3]$ (2)

A similar synthetic procedure was followed to isolate **2** like **1**, but $La(NO_3)_3.6H_2O$ was replaced with $Ce(NO_3)_3.6H_2O$ (0.1000 g, 0.23 mmol). Yield: 0.0220 g, 12.92 %. Elemental anal. calcd. : C, 42.17; H, 2.45; N, 17.02; found: C, 41.53; H, 2.20; N, 17.21. MALD-ToF-MS: m/z calcd for $C_{26}H_{19}N_9O_9Ce$ $[M+H]^+$ 741.037 g / mol ; found : 741.093 g / mol

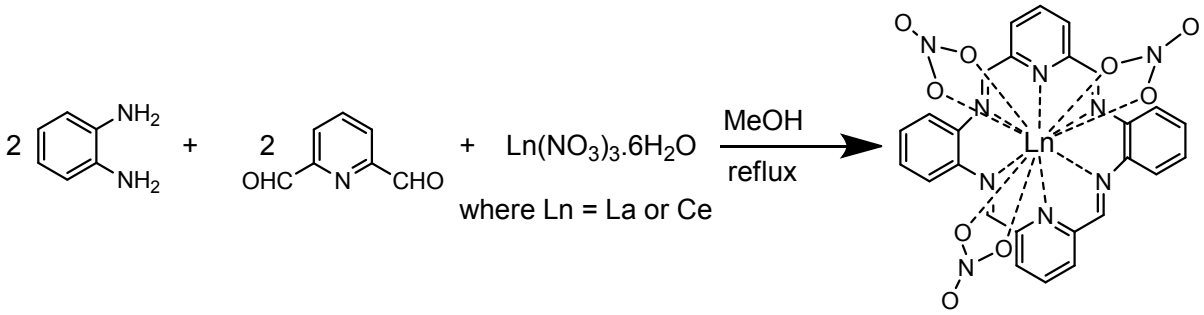

Scheme S1. General synthetic procedure followed to isolate **1** and **2**.

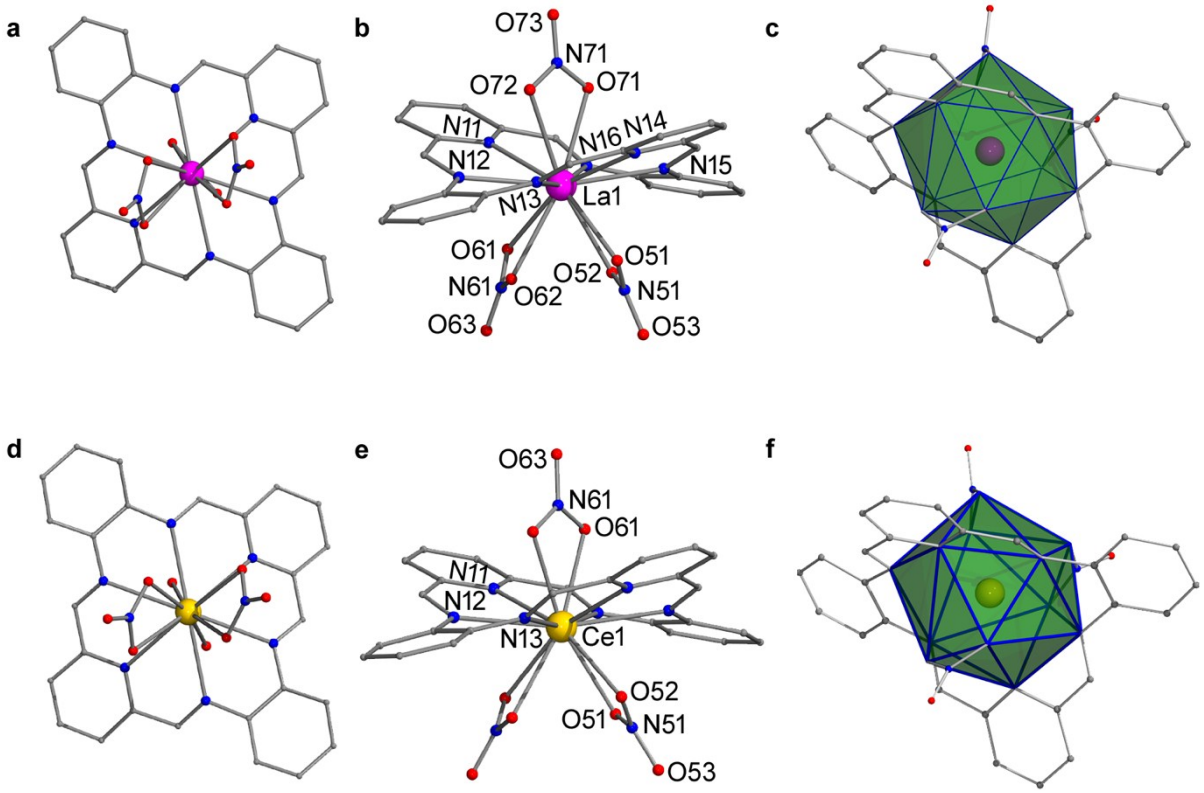

Figure S1. Ball and stick representation of the molecular structures. a,d) planar, b,e) side view and c, f) coordination polyhedron around metal of complexes **1** and **2** respectively. Colour code: Pink = La, Golden = Ce, Red = O, Blue = N, Grey = C.

Structural description of 1 and 2

The structure solution from X-ray diffraction reveals that both **1** and **2** are crystallized in the monoclinic unit cell with $P2_1/n$ and $C2/c$ space group respectively (Table S1). Although both **1** and **2** crystallized in different space group, both are structurally analogous to each other as seen from the representative crystal structure (Figure 1, Figure S1). From Figure 1, it is evident that the lanthanide salt facilitates the self-condensation of PC and PD resulting in a macrocyclic ligand L_1 (Scheme S1) which encapsulate Ln(III) ion. Detailed analysis of crystal structures of both **1** and **2** reveal that the L_1 is puckered with an average Ln_1-N bond length observed to be 2.738(5) Å and 2.735(3) Å for **1** and **2** respectively, unlike the other macrocyclic rings such as phthalocyanine that are planar.

In both complexes the average Ln1-O bond length (2.696(3) Å (for **1**), and 2.661(8) Å (for **2**) is slightly shorter than Ln1-N bond length in their respective complexes (Table S2). In both **1** and **2**, the lanthanide ion is surrounded by (O6N6) donor atoms and exhibit the Icosahedron geometry which is confirmed by continuous Shape Measurement (CShM) software.[2, 3]

Table S1. Crystallographic parameters for complexes **1** and **2**

	1	**2**
Formula	$C_{26}H_{18}N_9O_9La$	$C_{26}H_{18}N_9O_9Ce$
Size (mm)	0.064 × 0.318 × 0.300	0.214 × 0.062 × 0.048
System	Monoclinic	Monoclinic
Space group	$P2_1/n$	C2/c
a [Å]	9.1366(3)	15.0921(16)
b [Å]	14.1095(3)	10.8118(8)
c [Å]	20.9641(7)	19.5232(17)
β [°]	90.052(3)	118.320(13)
V [$Å^3$]	2702.53(13)	2804.4(5)
Z	4	4
ρ_{calcd} [g/cm^3]	1.817	1.754
$2\Theta_{max}$	50	50
Radiation	MoK_α	MoK_α
λ [Å]	0.71073	0.71073
T [K]	293(2)	293(2)
Reflns	9854	6863
Ind. Reflns	4657	2463
Reflns with >2σ(I)	4222	2078
R_1	0.0275	0.0509
wR_2	0.0690	0.1062

Table S2. Selected bond angle and bond distances for **1** and **2**

Bond length (Å)		
Label	**1**	**2**
Ln-O51	2.725(2)	2.657(4)
Ln-O52	2.679(2)	2.704(4)
Ln-O61	2.706(2)	2.621(10)
Ln-O62	2.716(2)	
Ln-O71	2.628(2)	
Ln-O72	2.715(2)	
Ln-N11	2.695(2)	2.713(5)
Ln-N12	2.742(2)	2.755(5)
Ln-N13	2.757(2)	2.736(5)
Ln-N14	2.738(3)	
Ln-N15	2.757(2)	
Ln-N16	2.727(2)	
Bond angle (°)		
	1	**2**
N11-Ln-N12	60.50(7)	60.3(13)
N12-Ln-N13	58.90(7)	58.3(13)
N13-Ln-N14	59.85(7)	
N14-Ln-N15	59.82(7)	
N15-Ln-N16	58.56(7)	
N16-Ln-N11	60.52(7)	
N11-Ln-N14	138.72(7)	
O51-Ln-O52	47.20(6)	47.7(13)
O61-Ln-O62	47.07(7)	
O71-Ln-O72	47.41(6)	
O51-Ln-O61	62.66(6)	124.0(17)
O52-Ln-O62	64.00(7)	
O51-Ln-O71	124.12(6)	
O51-Ln-O72	168.78(6)	164.8(3)
O52-Ln-O72	129.31(7)	
O52-Ln-O71	129.59(7)	
O62-Ln-O71	166.41(8)	
O62-Ln-O72	126.78(6)	
O61-Ln-O71	123.41(7)	
O61-Ln-O72	127.07(7)	

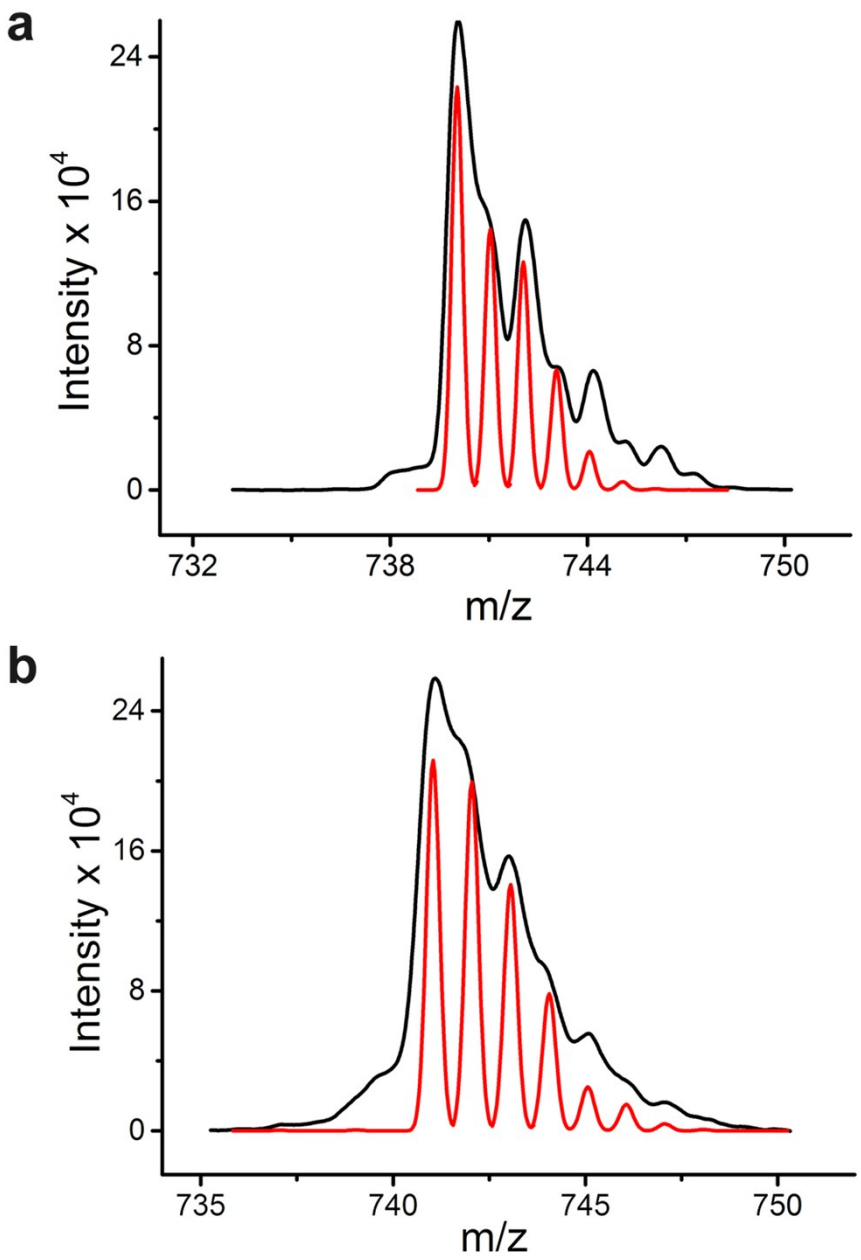

Figure S2. Stability of **1** and **2** in acetonitrile solution. a-b) MALDI-TOF traces of **1** and **2** respectively. Colour code: black for experimental and red is simulated for the combination of $[M+H]^+$, $[M+2H]^+$, $[M+3H]^+$ and $[M+4H]^+$ facilitated by presence of Schiff base group in the molecule.

GFET fabrication and functionalization steps

Commercially available graphene, grown by chemical vapor deposition, on polycrystalline Cu foil was transferred to Si substrate capped with 265 nm SiO_2 layer by means of Poly(methyl methacrylate) (PMMA) assisted wet transfer method. Such graphene transferred on Si/SiO_2 substrate is employed to fabricate back-gated field effect transistor structure with the graphene as channel and the Si substrate acting as the gate. The graphene channels were then patterned by optical lithography tool EVG620 and AZ5214E photoresist. Exposed graphene region was etched out by oxygen plasma using reactive ion etching technique. The source-drain contact pads are then patterned using optical lithography followed by electron-beam deposition of Ni/Au layer (~ 20 nm/ 50 nm). Thereby, an array of back-gated transistor structure with varying length and width have been fabricated as shown in Figure 2a. The femto liters of **1** and **2** dispensed spatially on graphene channel using FEMTOJET 4X injector. The sample is then baked for 15 minutes at 90 ^{o}C. Such non-covalently functionalized GFET is then utilized as n-type transistor of complementary inverter whereas non-functionalized GFET is used as p-type transistor.

Table S3. Electrical characterization for GFETs functionalized with **1** and **2**.

Device Parameters / Dopant	Time (in h)	Dirac Point (V)	Carrier Type	Carrier Density (/cm^2)	Transconductance g_m (μA/V)		Reference
					Hole	Electron	
Pristine Graphene	--	+4	Hole	3.25×10^{11}	6.0	1.4	This work
GFET + **1**	24	–10	Electron	8.13×10^{11}	6.8	5.5	
GFET + **1**	30	–14	Electron	1.14×10^{12}	6.5	5.2	
GFET + **1**	48	–18	Electron	1.46×10^{12}	7.5	5.5	
GFET + **1**	720	–18	Electron	1.46×10^{12}	8	8.8	
GFET + **1**	3600	–13	Electron	1.06×10^{12}	7.5	7.6	
GFET + **1**	7200	–22	Electron	1.79×10^{12}	7.3	6.1	
GFET + **2**	24	–20	Electron	1.63×10^{12}	9.8	6.4	
GFET + **2**	720	-13	Electron	1.06×10^{12}	9.6	8.4	
GFET + **2**	3600	–19	Electron	1.54×10^{12}	8.6	6.7	
GFET + P4VP	336	-17	Electron	1.22×10^{12}	59.5	40	[4]
GFET + 20wt% PVA	2520	-40	Electron	1.43×10^{13}	0.032	0.024	[5]
GFET + (N-DMBI)	720	-140	Electron	1.00×10^{12}	743	10051	[6]
GFET + PEI	12	-5	Electron	3.59×10^{11}	5.8	12	[7]
GFET + TETA	NA	-94	Electron	6.76×10^{12}	NA	0.51	[8]
GFET + TEPA	NA	-135	Electron	9.7×10^{12}	NA	0.336	[8]
GFET + PEHA	NA	-158	Electron	1.14×10^{13}	NA	0.291	[8]
GFET + PEI	NA	-58	Electron	4.17×10^{12}	NA	0.212	[8]
GFET + o-MeO-DMBI	240	-10	Electron	7.19×10^{12}	8.74	6.4	[9]
GFET + Selective electrical annealing at 3K	60 (stored at 3K)	2.1	Hole	1.50×10^{11}	--	--	[10]

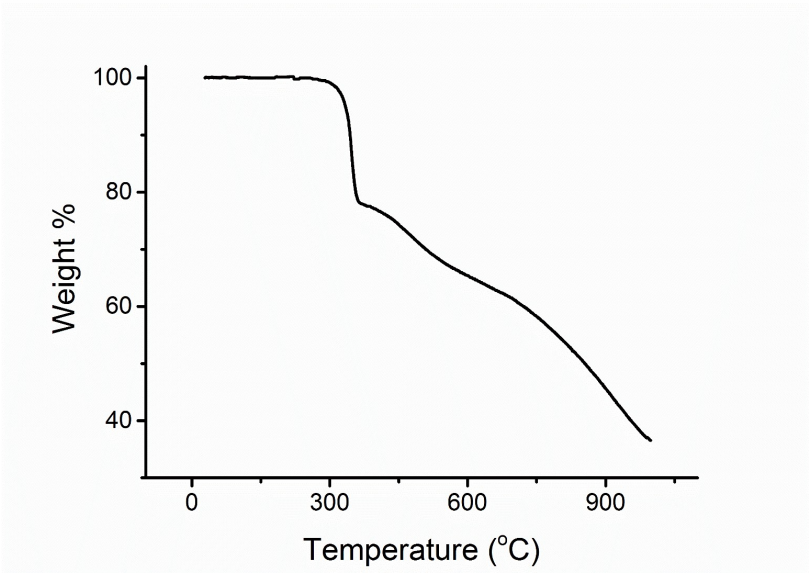

Figure S3. Thermo gravimetric analysis (TGA) of complex **2**

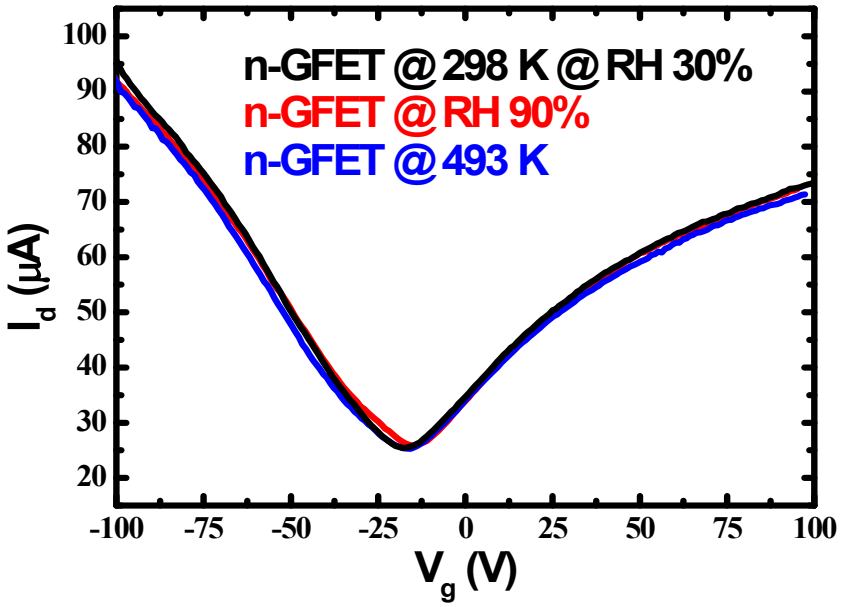

Figure S4. Transfer characteristic of n-GFET under different temperature (493 K) and relative humidity levels (RH 90%)

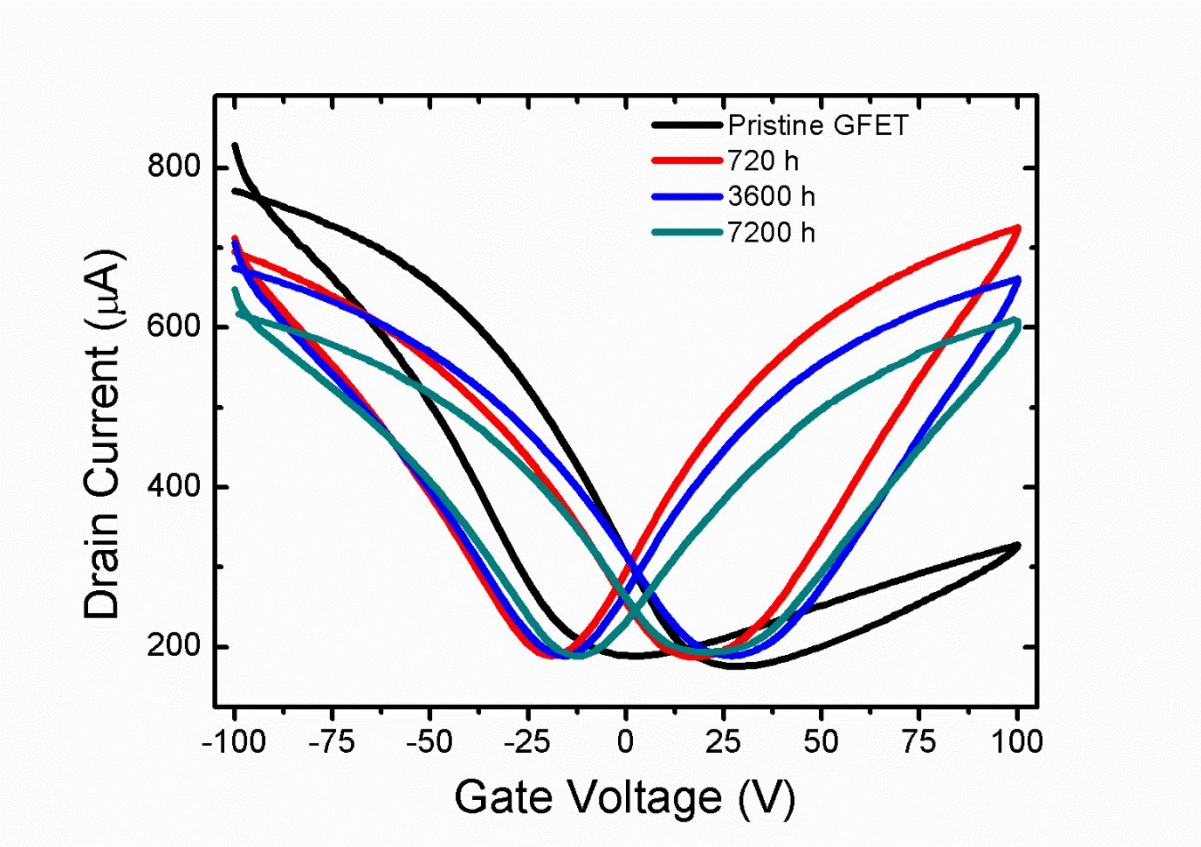

Figure S5. Time dependent variation of hysteresis curve for GFET functionalized with **1**.

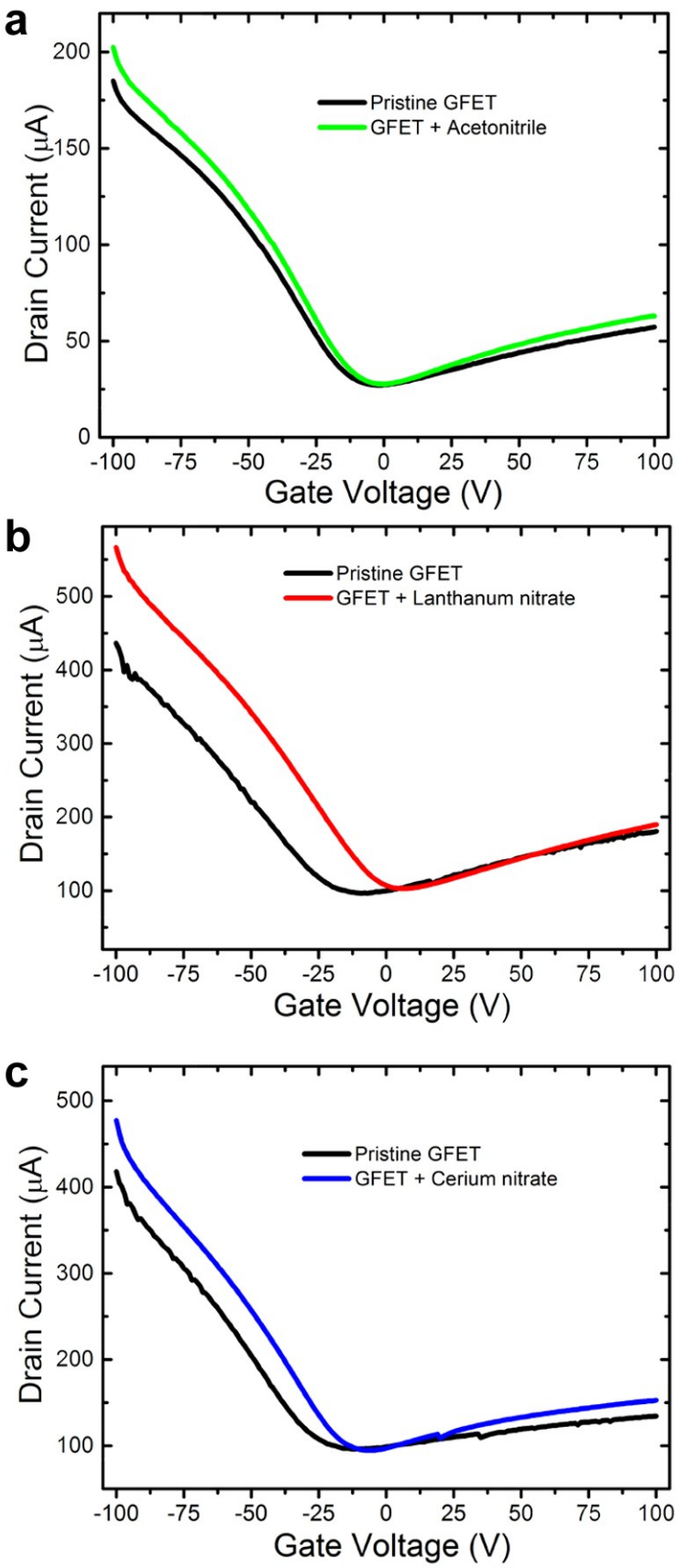

Figure S6. Control experiments. a-c) Electrical characteristic of pristine GFET and after treating it with acetonitrile, $La(NO_3)_3.6H_2O$ and $Ce(NO_3)_3.6H_2O$ respectively.

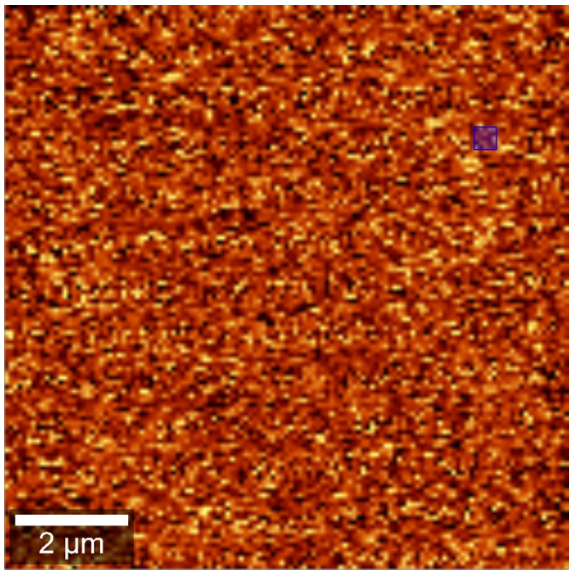

Figure S7. Raman spectral mapping of D peak of pristine GFET.

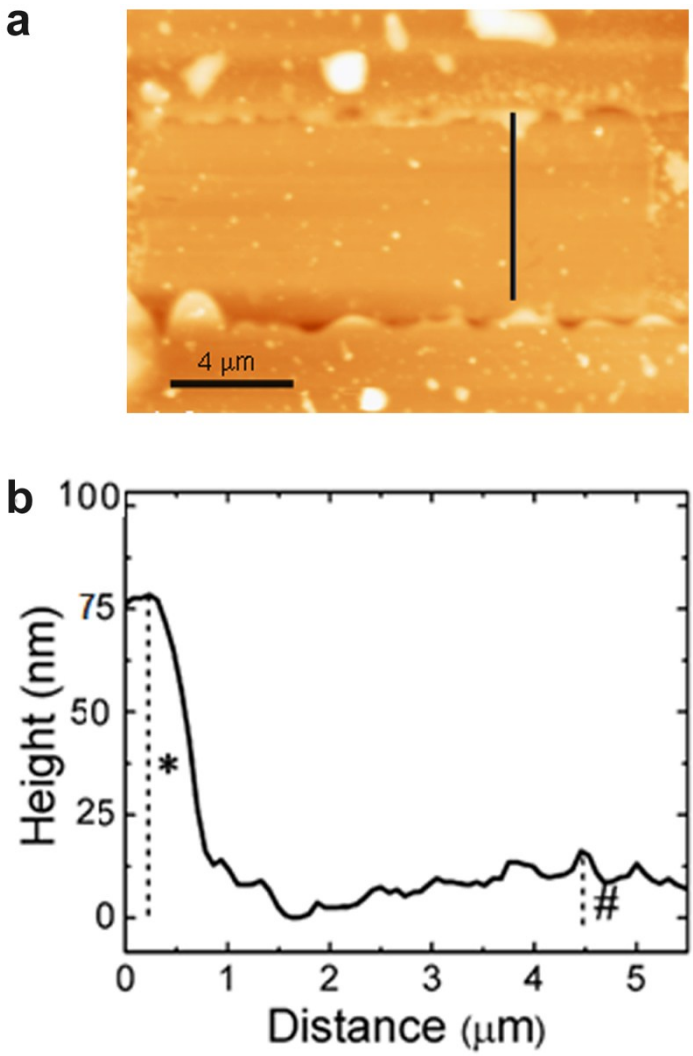

Figure S8. AFM study of GFET. a) AFM image of channel area of GFET. b) Height distribution of AFM image (* height of contact pad, # height of graphene layer).

	2 NO_3	1 NO_3	0 NO_3
	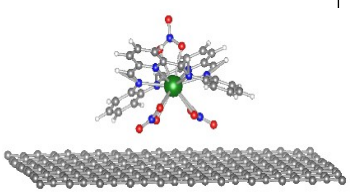	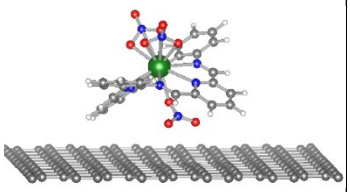	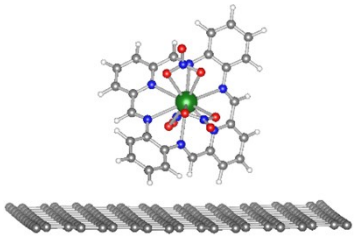
1 (eV)	0.0	0.75	0.90
2 (eV)	0.0	0.74	0.81

Figure S9. Optimized structures of **1** and **2** adsorbed on graphene sheet in different orientations along with their relative energies.

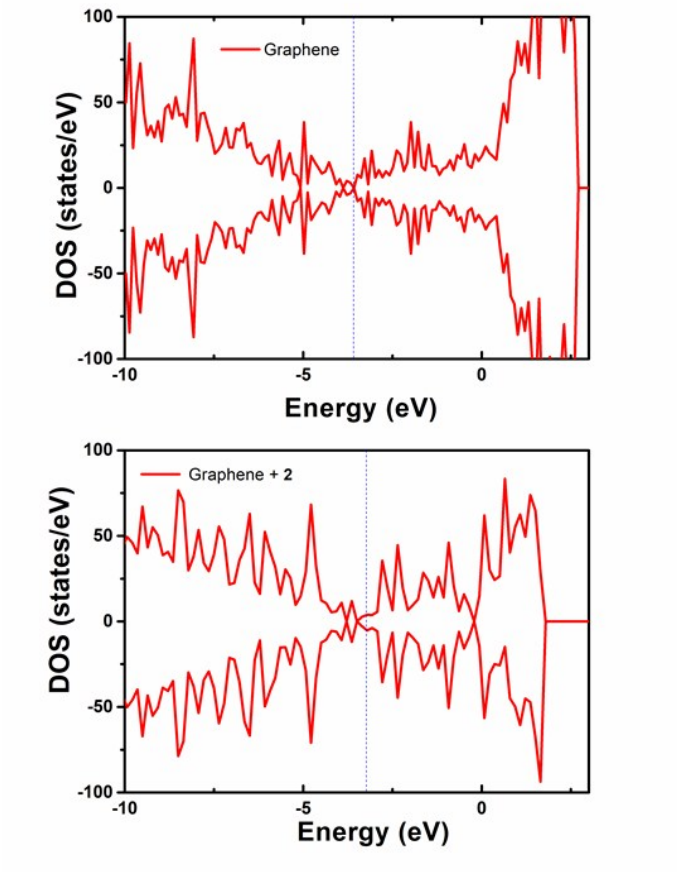

Figure S10. Computed density of state (DOS) plot. a) Total density of states of Stone-Wale defected graphene. b) Total density of states of Stone-Wale defected graphene functionalised with **2**.

Computational details

Kohn–Sham orbitals for the valence electrons are expanded using the plane-wave basis sets with a kinetic energy cut-off of 450 eV. Projector augmented wave (PAW) potentials were used to treat the ion–electron interactions.[11,12] For H, C, N, O, La and Ce, the valence states considered for construction of PAW potentials are [$1s^1$], [$2s^22p^2$], [$2s^22p^3$], [$2s^22p^4$], [$5s^25p^64f^05d^16s^2$] and $5s^25p^64f^15d^16s^2$ respectively. Graphene sheet has been considered in the YZ-plane with 30 Å vacuum along the X-direction. All the structures were optimized at constant volume with a force cutoff of 0.01 eV/Å. Only Γ is considered for the optimizations

whereas 1 x 9 x 9 Monkhorst–Pack set of k-points were used for the calculation of density of states (DOS).[13] The exchange–correlation energy functional, Exc[r] has been obtained by using the Generalized Gradient Approximation (GGA) of Perdew–Burke–Ernzerhof (PBE).[14] p4vasp[15] and VESTA[16] were used for analyzing the results and generating the reported figures.

Initial calculations were performed on pristine graphene for three possible orientations. The calculated adsorption energy for the minimum energy structure is found to be -0.928 eV and -0.835 eV for **1** and **2** respectively. The shortest C-O distance is measured to be 3.0 Å indicating strong interaction between the macrocyclic complexes and graphene substrate. As a result of this interaction, the carbon atoms in the graphene surface are slightly distorted compared to the optimized pristine graphene structure. These structural changes and strong interaction energies indicate a strong π-π as well as C-H…π interactions between the macrocyclic ligand of the complex and graphene surface. Comparing the binding energy computed with other n-dopant heterocyclic molecules on graphene reveal that the binding energy is comparable to the organic molecules such as aniline and 2-aminopyridine. A similar set of energies have been obtained for both **1** and **2**, hence we consider here only **2** for further discussion. Calculations reveal that the molecule adsorbed on the pristine graphene surface exhibit weak n-type character.

References

1. F. Hamon, E. Largy, A. Guédin-Beaurepaire, M. Rouchon-Dagois, A. Sidibe, D. Monchaud, J. L. Mergny, J. F. Riou, C. H. Nguyen and M. P. Teulade-Fichou, *Angew. Chem. Int. Ed.,* 2011, **123**, 8904-8908.
2. D. H. Rouvray, *Concepts in Chemistry: A Contemporary Challenge*, Research Studies Press, 1997.
3. H. Zabrodsky, S. Peleg and D. Avnir, *J. Am. Chem. Soc.,* 1992, **114**, 7843-7851.
4. J. M. Yun, S. Park, Y. H. Hwang, E.-S. Lee, U. Maiti, H. Moon, B.-H. Kim, B.-S. Bae, Y.-H. Kim and S. O. Kim, *ACS Nano*, 2013, 8, 650-656.
5. S. Kim, P. Zhao, S. Aikawa, E. Einarsson, S. Chiashi and S. Maruyama, *ACS Appl. Mater. Interfaces*, 2015, **7**, 9702-9708.

6. W. Xu, T. S. Lim, H. K. Seo, S. Y. Min, H. Cho, M. H. Park, Y. H. Kim and T. W. Lee, *Small*, 2014, **10**, 1999-2005.
7. Y. Choi, Q. Sun, E. Hwang, Y. Lee, S. Lee and J. H. Cho, *ACS Nano*, 2015, **9**, 4354-4361.
8. I. Jo, Y. Kim, J. Moon, S. Park, J. San Moon, W. B. Park, J. S. Lee and B. H. Hong, *Phys. Chem. Chem. Phys.*, 2015, **17**, 29492-29495.
9. P. Wei, N. Liu, H. R. Lee, E. Adijanto, L. Ci, B. D. Naab, J. Q. Zhong, J. Park, W. Chen and Y. Cui, *Nano Lett.*, 2013, **13**, 1890-1897.
10. F. Traversi, V. Russo and R. Sordan, *Appl.Phys. Lett.*, 2009, **94**, 150.
11. G. Kresse and D. Joubert, *Phys. Rev. B*, 1999, **59**, 1758.
12. P. E. Blöchl, *Phys. Rev. B*, 1994, **50**, 17953.
13. H. J. Monkhorst and J. D. Pack, *Phys. Rev. B*, 1976, **13**, 5188.
14. J. P. Perdew, K. Burke and M. Ernzerhof, *Phys. Rev. Lett.*, 1996, **77**, 3865.
15. http://www.p4vasp.at/#/.
16. K. Momma and F. Izumi, *J. Appl.Crystallogr.*, 2008, **41**, 653-658.